Case Studies in Chemical and Environmental Engineering 11 (2025) 101088

Contents lists available at ScienceDirect

Case Studies in Chemical and Environmental Engineering

journal homepage: www.sciencedirect.com/journal/case-studies-in-chemical-and-environmental-engineering

Case Report

Thermodynamic modeling of calcium sulfate hemihydrate formed from seawater and concentrated brine at elevated temperature

Ali Al-Hamzah [a,b], Caillan J. Fellows [c], Christopher M. Fellows [a,b,*]

[a] Water Technologies Innovation Institute and Research Advancement, Saudi Water Authority, Al Jubail, Kingdom of Saudi Arabia
[b] School of Science and Technology, The University of New England, NSW, 2351, Australia
[c] School of Economics, Business and Law, The University of New England, NSW, 2351, Australia

ARTICLE INFO

Keywords:
Hard scale
Calcium sulfate hemihydrate
Multi-stage flash desalinatio
Gibbs free energy
Solubility product
Pitzer model

ABSTRACT

Formation of hard scale, predominantly calcium sulfate, is the limiting factor in the operation of multi-stage flash (MSF) thermal desalination of seawater, restricting the top temperature and top brine concentration that can be achieved. More accurate prediction of the solubility product of calcium sulfate hemihydrate, the scaling species formed initially above 100 °C, under conditions found in MSF plants, would allow better control of MSF operations. In this report literature data for calcium sulfate solubility is analysed and the Pitzer model applied to determine solubility product values at temperatures up to 148 °C and total dissolved solids concentration up to 99 g/L (equivalent to a concentration factor for Arabian Gulf seawater of 2.2). From these an analytical expression is determined for predicting the supersaturation index (SI) under these conditions to simplify the task of MSF plant operators, SI = 61.5891–0.4783 ln(TDS) + 0.3223 $(\ln(TDS))^2$–31.7890 ln(T) + 3.7977 $(\ln(T))^2$

1. Introduction

Thermal desalination of seawater has historically been the primary source of potable water in the Gulf Cooperation Council (GCC) region and the multi-stage flash (MSF) process still provides a large proportion of water for domestic and industrial consumption in the GCC. The top brine temperature (TBT) of the MSF process determines the extent of recovery and energy efficiency: the higher the TBT, the more economical the process. However, TBT is limited by the formation by inverse solubility salts of intractable hard scale, of which calcium sulfate is the dominant component [1–4]. If formation of this calcium sulfate scale can be avoided, MSF can be operated at higher temperatures, giving greater recovery and higher energy efficiency [5]. Calcium sulfate can exist as one of three different hydrates. Gypsum ($CaSO_4.2H_2O$, density = 2.32 g.cm^{-3}), is the form whose formation is thermodynamically favourable below 100 °C, whereas calcium sulfate hemihydrate ($CaSO_4.1/2H_2O$, density = 2.74 g.cm^{-3}) or anhydrite ($CaSO_4$, density = 2.96 g.cm^{-3}) deposit at higher temperatures (Eqs. (1) and (2)). While anhydrite is the thermodynamically-favoured state above 100 °C, under most desalination conditions its induction period is much longer than the induction period of the hemihydrate [6].

$$CaSO_4.2H_2O \xrightarrow{\Delta} CaSO_4.\frac{1}{2}H_2O + \frac{3}{2}H_2O \text{ Fast at } T = 98\ ^\circ C \quad \text{Eq. 1}$$

$$CaSO_4.\frac{1}{2}H_2O + \frac{3}{2}H_2O \xrightarrow{\Delta} CaSO_4 + 2\,H_2O \text{ Slow at } T > 98\ ^\circ C \quad \text{Eq. 2}$$

Whatever the species formed, the resulting calcium sulfate scales are typically hard and adherent, making them difficult and costly to remove [1,2].

The variation of solubility of calcium sulfate species with temperature has been studied by a number of investigators [3,7–13]. Due to the relatively slow crystallization kinetics of the system, there are significant uncertainties in the phase solubility diagram of $CaSO_4$ [14,15], but the general features of the system may be seen in Fig. 1. This figure displays the solubility data summarized by Partridge and White between 0 and 150 °C [16].

It can be seen that the solubilities of all calcium sulfate polymorphs decrease with increasing temperature except for gypsum ($CaSO_4{\cdot}2H_2O$) below 42 °C. In thermal desalination processes, the most critical phase is calcium sulfate hemihydrate, the kinetically-favoured product at all temperatures on interest, rather the thermodynamically-favoured calcium sulfate anhydrite or dihydrate, as the kinetics of its transition to the thermodynamically-favoured form(s) are slow [15,17], with an activation energy of about 40 kJ/mol [18]. There is evidence that carboxylate

* Corresponding author. Water Technologies Innovation Institute and Research Advancement, Saudi Water Authority, Al Jubail, Kingdom of Saudi Arabia.
E-mail address: cfellows@une.edu.au (C.M. Fellows).

https://doi.org/10.1016/j.cscee.2024.101088
Received 22 October 2024; Received in revised form 20 November 2024; Accepted 28 December 2024
Available online 31 December 2024

additives, such as the polymeric antiscalants commonly employed in thermal desalination, can retard this transition further [18–20].

MSF plants currently operate at a TBT under 120 °C to keep brine solution under supersaturation with respect to calcium sulfate formation. Increase of TBT to 130 °C resulted in a 48 % increase in water production [21], but in practice the temperature accessible for realistic feed waters is limited by the solubility of calcium sulfate salts. Two possible viable approaches exist for increasing TBT of thermal plants. The first approach is to remove calcium, magnesium, bicarbonate and sulfate ions from the raw seawater by pretreatment using a nanofiltration membrane [22]. Another approach is development of scale inhibitors that can operate effectively at 125–140 °C [23].

A hybrid desalination process using a combination of nanofiltration pre-treatment with MSF (NF-MSF) and MED (NF-MED) to increase TBT to 140 °C has been proposed by Hamed et al. [24]. Application of this process requires knowledge of the thermodynamics of solubility product K_{sp} for $CaSO_4.1/2H_2O$, the first calcium sulfate to precipitate (Eq. (1)), at different temperatures and total dissolved solids content (TDS). To control operating conditions within the MSF and MED pilot plants at WTIIRA, we initially used the extended Debye-Hückel model to estimate the activity coefficients of Ca^{2+} and SO_4^{2-}. The extended Debye-Hückel model is not appropriate above an ionic strength of 0.5 M, and desalination brines are well above this level, so we have more recently applied the Pitzer model by preference. Using this model, we have derived semi-empirical polynomial expressions for the scaling limits as a function of brine temperature and total dissolved solids (TDS).

2. Pitzer model for calcium sulfate hemihydrate ($CaSO_4.1/2H_2O$)

The Pitzer Model is the most comprehensive model for the estimation of activity coefficients at high ionic strength ($I < 6$ m) and temperature ($T \leq 250$ °C) [25]. It takes into account many parameters, such as ionic strength, temperature, chemical composition, electrostatic effects and short and long ion interaction forces. For seawater, the Pitzer model requires stability constants for seven ion complexes HSO_4^-, HF, MgF^+, CaF^+, $MgOH^+$, $MgCO_3$ and $CaCO_3$. It will be applied in this work to estimate activity coefficients in seawater.

In this work the Pitzer model was used to estimate the activity coefficients of Ca^{2+} and SO_4^{2+} and activity of H_2O over ranges of elevated temperatures (100–148 °C) and different TDS values (45,000–99,000 mg/L) corresponding to potential MSF and MED desalination plant operating conditions. The activity coefficients calculated for those ions were then used to calculate the solubility product K_{sp} and ionic product Q_{IP} of $CaSO_4.1/2H_2O$ (Equation (3)).

$$K_{sp} = \gamma_{Ca^{2+}} \left[Ca^{2+}\right]_{sat} \times \gamma_{SO_4^{2-}} \left[SO_4^{2-}\right]_{sat} \times (a_{H2O})^{0.5} \quad \text{Eq. 3a}$$

$$Q_{IP} = \gamma_{Ca^{2+}} \left[Ca^{2+}\right] \times \gamma_{SO_4^{2-}} \left[SO_4^{2-}\right] \times (a_{H2O})^{0.5} \quad \text{Eq. 3b}$$

Where a_{H2O} is the activity of H_2O, γ_{Ca}^{2+} and γ_{SO4}^{2-} are the activity coefficient of Ca^{2+} and SO_4^{2-} respectively. The activity coefficient values of Ca^{2+} and SO_4^{2-} vary markedly with temperature and TDS, which will lead to dramatically different K_{sp} values under different conditions [26–28].

The Pitzer model was used to calculate the activity of H_2O and the activity coefficient of Ca^{2+} and SO_4^{2-} at different temperatures and TDS as follows:

$$ln(\gamma_{Ca^{2+}}) = 4f^{\gamma} + 2m_{Cl}(B_{CaCl_2} + m_{Na}C_{CaCl_2}) + 4m_{Na}\,m_{Cl}\,B'_{NaCl} + 2m_{Na}\,m_{Cl}\,C_{NaCl} + m_{Na}(2\Theta_{Na-Ca} + m_{Cl}\Psi_{Na-Ca-Cl}) \quad \text{Eq. 4}$$

$$ln\left(\gamma_{SO_4^{4-}}\right) = 4f^{\gamma} + 2m_{Na}\left(B_{Na_2SO_4} + m_{Cl}C_{Na_2SO_4}\right) + 4m_{Na}\,m_{Cl}\,B'_{NaCl} + 2m_{Na}\,m_{Cl}C_{NaCl} + m_{Cl}\left(2\Theta_{Cl-SO_4} + m_{Na}\Psi_{Cl-SO_4-Na}\right) \quad \text{Eq. 5}$$

Where f^{γ} is the Debye-Hückel term (Eqs. (8) and (9)), m_i is the molality of species i, B_{MX}, B'_{MX} and C_{MX} are the Pitzer terms for ionic strength dependence (Eqs. (10)–(12)) and $\beta^{(0)}_{NaCl}$, $\beta^{(1)}_{NaCl}$ and C^{ϕ}_{NaCl} are the Pitzer terms for temperature dependence (Eq. (13)). $\Theta_{i\text{-}j}$ are interactions for like charge ions (0.07 for both $\Theta_{Na\text{-}Ca}$ and $\Theta_{Cl\text{-}SO4}$) and $\Psi_{i\text{-}j\text{-}k}$ are triplet interaction terms (−0.007 for $\Psi_{Na\text{-}Ca\text{-}Cl}$ and −0.009 for $\Psi_{Na\text{-}Ca\text{-}SO4}$) [29].

The activity of water in equation (3) was estimated by:

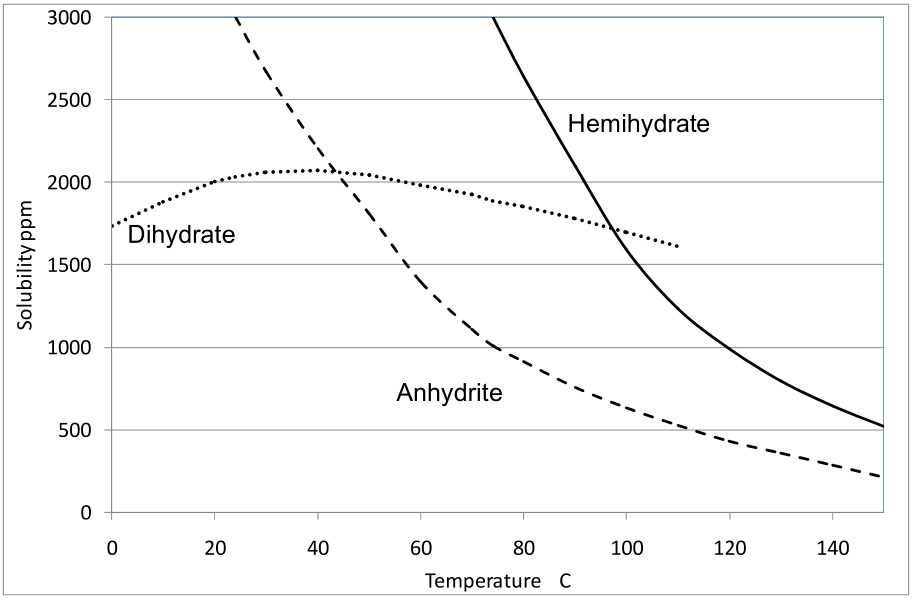

Fig. 1. Experimental solubilities of the three principal hydrates of calcium sulfate [16].

$$\ln a(H_2O) = -\left(\frac{2\,m_{NaCl}}{m\mathrm{H2O}}\right)\varnothing \quad \text{Eq. 6}$$

Where ∅ is given by:

$$\varnothing = 1 + f^{\varnothing} + m_{Na}B^{\varnothing}_{NaCl} + m_{Na}m_{Cl}C^{\varnothing}_{NaCl} \quad \text{Eq. 7}$$

f^{γ} in Eqs. (4) and (5) is the Debye-Hückel term as follows:

$$f^{\gamma} = -A_{\varnothing}\left[\frac{I^{0.5}}{(1+1.2I^{0.5})} + \frac{2}{1.2}\ln\left(1+1.2I^{0.5}\right)\right] \quad \text{Eq. 8}$$

Where values of $A_{\varnothing}$ valid from 0 to 350 °C are given by [30]:

$$A_{\varnothing} = 0.36901532 - 6.32100430\times10^{-4}T + \frac{9.14252359}{T} - 1.35143986 \times 10^{-2}lnT + \frac{2.26089488\times10^{-3}}{T-263} + 1.92118597\times10^{-6}\,T^2 + \frac{45.2586464}{680-T} \quad \text{Eq. 9}$$

2.1. Pitzer parameters for ionic strength dependence

The values of Pitzer parameters for ionic strength dependence (B_{MX}, B'_{MX} and C_{MX}) for NaCl as a 1:1 electrolyte and Na_2SO_4 and $CaCl_2$ as 2:1 electrolytes in Eqs. (10) and (11) are given as follows:

$$B_{MX} = \beta'_{MX} + \left(\frac{\beta^1_{MX}}{2I}\right)\left[1-(1+2I^{0.5})\exp(-2I^{0.5})\right] \quad \text{Eq. 10}$$

$$B'_{MX} = \left(\frac{\beta^1_{MX}}{2I^2}\right)\left[-1+\left(1+2I^{0.5}+2I\exp(-2I^{0.5})\right)\right] \quad \text{Eq. 11}$$

$$C_{MX} = \frac{C^{\phi}_{MX}}{\left(2|Z_MZ_X|^{0.5}\right)} \quad \text{Eq. 12}$$

$$B^{\varnothing}_{NaCl} = \beta^{\circ}_{NaCl} + \beta^1_{NaCl}\,exp(-2I^{0.5}) \quad \text{Eq. 13}$$

Ionic strength was calculated from salinity S and density ρ using the empirical expression I = 0.019915(S/ρ)/(1 − 1.00487(S/ρ)) [31]. Salinity (g/L) was in turn determined from TDS (g/L) using the expression S = TDS/1.004715 based on the typical proportion of carbonate species in seawater. Solution density was determined as a function of temperature and TDS using http://www.csgnetwork.com/h2odenscalc.html.

2.2. Pitzer parameters for temperature dependence

The values of Pitzer parameters for temperature dependence ($\beta^{(0)}_{NaCl}$, $\beta^{(1)}_{NaCl}$ and C^{ϕ}_{NaCl}) for NaCl and $CaCl_2$ are given by Eq. (14).

$$P(T) = a_1 + a_2T + \frac{a_3}{T} + a_4\,ln\,T + \frac{a_5}{T-263} + a_6T^2 + \frac{a_7}{680-T} + \frac{a_8}{T-227} \quad \text{Eq. 14}$$

Where P is equal to $(\beta^{(O)}_{NaCl}, \beta^{(1)}_{NaCl}\ and\ C^{\varphi}_{NaCl})$

The values of parameters a_1, a_2, a_3, a_4, a_5, a_6, a_7 and a_8 for NaCl and $CaCl_2$ are given by Møller [30] and Greenberg and Møller [32] from 0 to 250 °C (Tables A2 and A3).

The Pitzer coefficient values for temperature dependence, $\left(\beta^{(O)}_{Na_2SO_4}, \beta^{(1)}_{Na_2SO_4}\ and\ C^{\varphi}_{Na_2SO_4}\right)$ for Na_2SO_4 are given by Eq. 15

$$P = a + b\left(\frac{1}{T} - \frac{1}{298.15}\right) + c\ln\left(\frac{T}{298.15}\right) \quad \text{Eq. 15}$$

The value of parameters a, b and c of Na_2SO_4 available in the literature (e. g., Pierrot et al. [33], Millero and Pierrot [28]) are only valid up to 100 °C. Moreover, most references only present accurate values of $\beta^{(O)}_{Na_2SO_4}, \beta^{(1)}_{Na_2SO_4}\ and\ C^{\varphi}_{Na_2SO_4}$ at 25 °C (e.g., Sheikholeslami & Ong, [34]; Simoes et al. [35]), although values at 25, 50, 100 and 150 °C are presented in Pitzer [25]. In the current study, the values of parameters a, b and c for Pitzer coefficient temperature dependence $\left(\beta^{(O)}_{Na_2SO_4}, \beta^{(1)}_{Na_2SO_4}\ and\ C^{\varphi}_{Na_2SO_4}\right)$ of Na_2SO_4 were estimated based on the values at 25, 100 and 150 °C presented by Pitzer [25] to extend their validity over a wider range of temperature and calculate absolute values at the temperatures of interest (112, 124, 136 and 148 °C).

The parameter a is temperature-independent (Eq. (15)), therefore its value is equal to the value of $\left(\beta^{(O)}_{Na_2SO_4}, \beta^{(1)}_{Na_2SO_4}\ and\ C^{\varphi}_{Na_2SO_4}\right)$ at 25 °C given by Pitzer [25]. The parameters b and c can be estimated by the substitution value of $\left(\beta^{(O)}_{Na_2SO_4}, \beta^{(1)}_{Na_2SO_4}\ and\ C^{\varphi}_{Na_2SO_4}\right)$ at certain T in Eq. (15).

For example, the parameters b and c of $\beta^{(1)}_{Na_2SO_4}$ at 100 and 150 °C can be estimated by using Eq. (15) and its values at these temperatures as follows:

At 25 °C

$$\beta^{(1)}_{Na_2SO_4} = 1.0559,$$

At 100 °C,

$$\beta^{(1)}_{Na_2SO_4} = 1.3421, \text{giving} \quad \text{Eq. 16a}$$

$$1.3421 = 1.0559 + b\left(\frac{1}{373.15} - \frac{1}{298.15}\right) + c\ln\left(\frac{373.15}{298.15}\right) \quad \text{Eq. 16b}$$

At 150 °C,

$$\beta^{(1)}_{Na_2SO_4} = 1.5710, \text{giving} \quad \text{Eq. 17a}$$

$$1.5710 = 1.0559 + b\left(\frac{1}{423.15} - \frac{1}{298.15}\right) + c\ln\left(\frac{423.15}{298.15}\right) \quad \text{Eq. 17b}$$

b and c can be determined by solving Eq. (16) and Eq. (17).

The values of parameters a, b and c of $\beta^{(O)}_{Na_2SO_4}, \beta^{(1)}_{Na_2SO_4}\ and\ C^{\varphi}_{Na_2SO_4}$ are tabulated in Table 1. The comparison between values of $\beta^{(O)}_{Na_2SO_4}$, $\beta^{(1)}_{Na_2SO_4}\ and\ C^{\varphi}_{Na_2SO_4}$ calculated in this study and their literature values are tabulated in Table 2 at 100 and 150 °C covering the temperature range of interest to this study.

3. Results and discussion

The results for estimation of activity coefficient (γ) of Ca^{2+} and SO_4^{2-} and K_{sp} of $CaSO_4.1/2H_2O$ showed γ and K_{sp} decreasing as expected with increasing temperature (from 100 to 148 °C) and increasing concentration factor (CF) (from 1.0 to 2.2 based on TDS = 45,000 mg/L for Arabian Gulf seawater) as shown in Table 3 and Figs. 2 and 3.

In thermal desalination processes, the goal should be to keep the brine solution under supersaturation with respect to $CaSO_4.1/2H_2O$ formation to make that approach more economic at certain conditions like TDS and temperature. For example, the ion product (Q_{IP}) of

Table 1
Values of parameters a, b and c for Pitzer coefficient temperature dependence $\left(\beta^{(O)}_{Na_2SO_4}, \beta^{(1)}_{Na_2SO_4}\ and\ C^{\varphi}_{Na_2SO_4}\right)$ of Na_2SO_4.

Parameter	$\beta^{(O)}_{Na_2SO_4}$	$\beta^{(1)}_{Na_2SO_4}$	$\beta^{(2)}_{Na_2SO_4}$	$C^{\varphi}_{Na_2SO_4}$
A	0.0181	1.0559	0.0	0.00202
B	−125.284	1122.64	0.0	23.602
C	0.00152653	4.64838	0.0	0.0438

Table 2
Comparison between values of $\beta^{(O)}_{Na_2SO_4}, \beta^{(1)}_{Na_2SO_4}$ *and* $C^{\phi}_{Na_2SO_4}$ calculated in this study and values in Pitzer [25] at 100 and 150 °C.

Pitzer coefficient temperature dependent	This study		Values from Pitzer	
	100 °C	150 °C	100 °C	150 °C
$\beta^{(O)}_{Na_2SO_4}$	0.1029	0.1427	0.1029	0.1227
$\beta^{(1)}_{Na_2SO_4}$	1.3421	1.5711	1.3421	1.5710
$C^{\phi}_{Na_2SO_4}$	−0.0041	−0.0060	−0.0041	−0.0060

Table 3
Ion product (Q_{IP}) and solubility product (K_{sp}) for $CaSO_4.1/2H_2O$ at different temperatures and CF = 1.4, TDS = 63,000 mg/L.

T (°C)	Q_{IP}	K_{sp}	Q_{IP}/K_{sp}
100	5.65×10^{-6}	1.15×10^{-5}	0.49
112	4.88×10^{-6}	6.56×10^{-6}	0.74
124	4.13×10^{-6}	3.59×10^{-6}	1.15
136	3.44×10^{-6}	1.86×10^{-6}	1.85
148	2.80×10^{-6}	9.22×10^{-7}	3.03

$CaSO_4.1/2H_2O$ at CF = 1.4 (TDS = 63,000 mg/L) at different temperatures was calculated using Eq. (3) based on the concentration of Ca^{2+} and SO_4^{2-} proposed by Zannoni et al. [36] and the activity of H_2O and activity coefficient of Ca^{2+} and SO_4^{2-} obtained by this study. If Q_{ip}/K_{sp} is less than 1, the solution is below saturation and scale formation is not expected. If Q_{ip}/K_{sp} is greater than 1, then the solution is above saturation and scale formation is thermodynamically favourable, although it may not proceed at an appreciable rate depending on the environmental conditions. The given brine solutions were found to be below saturation with respect to $CaSO_4.1/2H_2O$ formation at 100 °C ($Q_{IP}/K_{sp} = 0.49$) and 112 °C ($Q_{IP}/K_{sp} = 0.74$) (Table 3). Q_{IP}/K_{sp} further increases to 1.15 at 124 °C, indicating the pronounced inverse solubility of $CaSO_4.1/2H_2O$ with increasing temperature. These results correlate extremely well with observed behaviour in MSF plant operations where a maximum CF of 1.4 is standard and significant $CaSO_4.1/2H_2O$ scaling typically first becomes observable at about 120–122 °C, approximately the location where $Q_{IP}/K_{sp} = 1$ at the corresponding temperature [37].

Fig. 4(a) displays the overall variation in Q_{IP}/K_{sp} with temperature and concentration. An alternative way of presenting this data is in terms of the overall Gibbs Free Energy change of the reaction ΔG, where $\Delta G = \Delta G^{\circ} - RT\ln Q_{IP}$ and $\Delta G^{\circ} = -RT\ln K_{sp}$ (Fig. 4(b)) ($R = 8.314\ JK^{-1}mol^{-1}$, T in K).

A formula was fitted to the supersaturation data to provide a simple estimator of scaling potential as a function of temperature and TDS, using a supersaturation index (SI) defined as the log of the ratio of the ion product to the solubility product, Q_{ip}/K_{sp}. The equation was obtained using a multiple linear regression, which was optimised minimising the maximum absolute deviation.

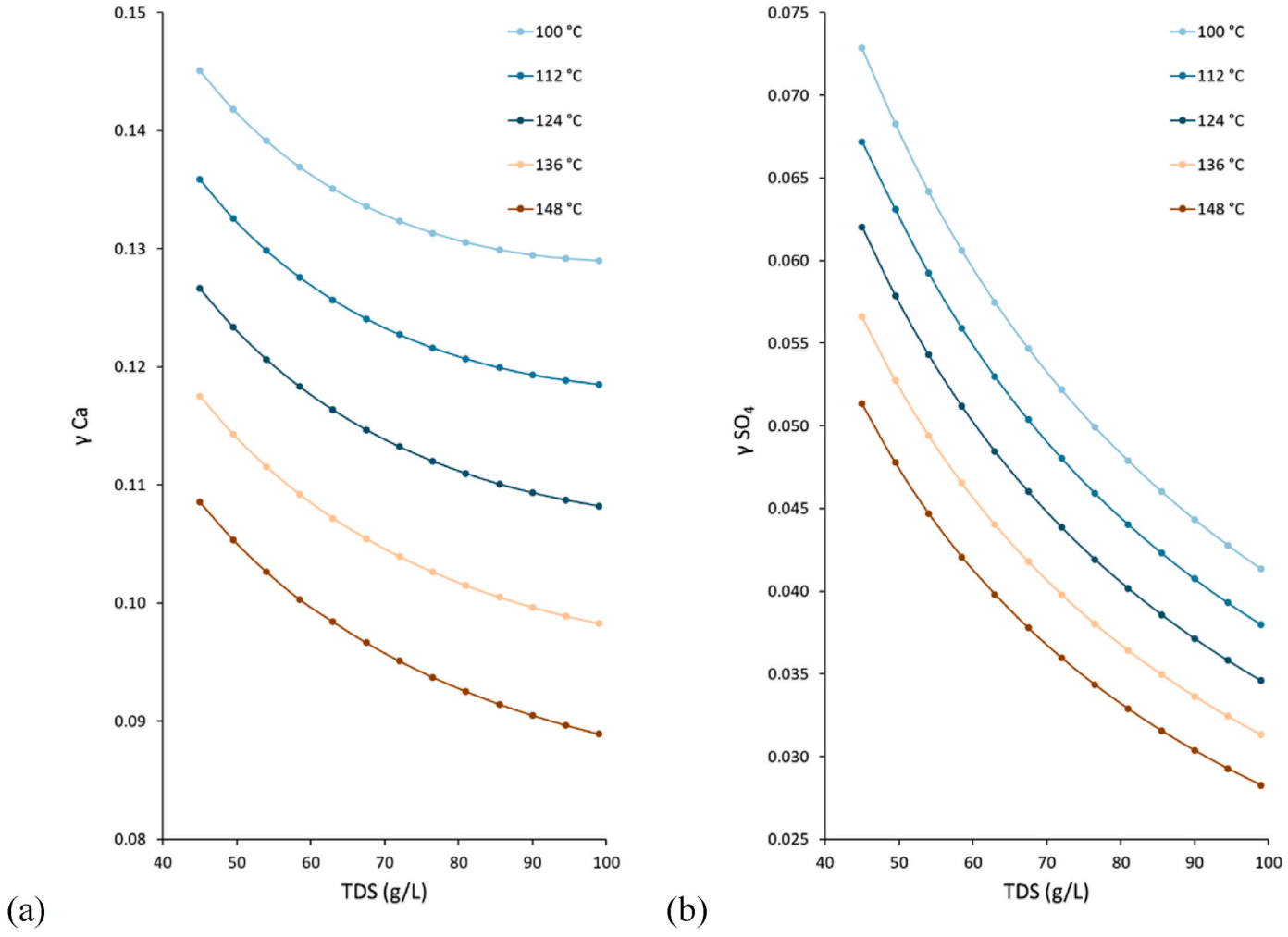

Fig. 2. Activity coefficients for (a) Ca^{2+} and (b) SO_4^{2-} calculated by the Pitzer model.

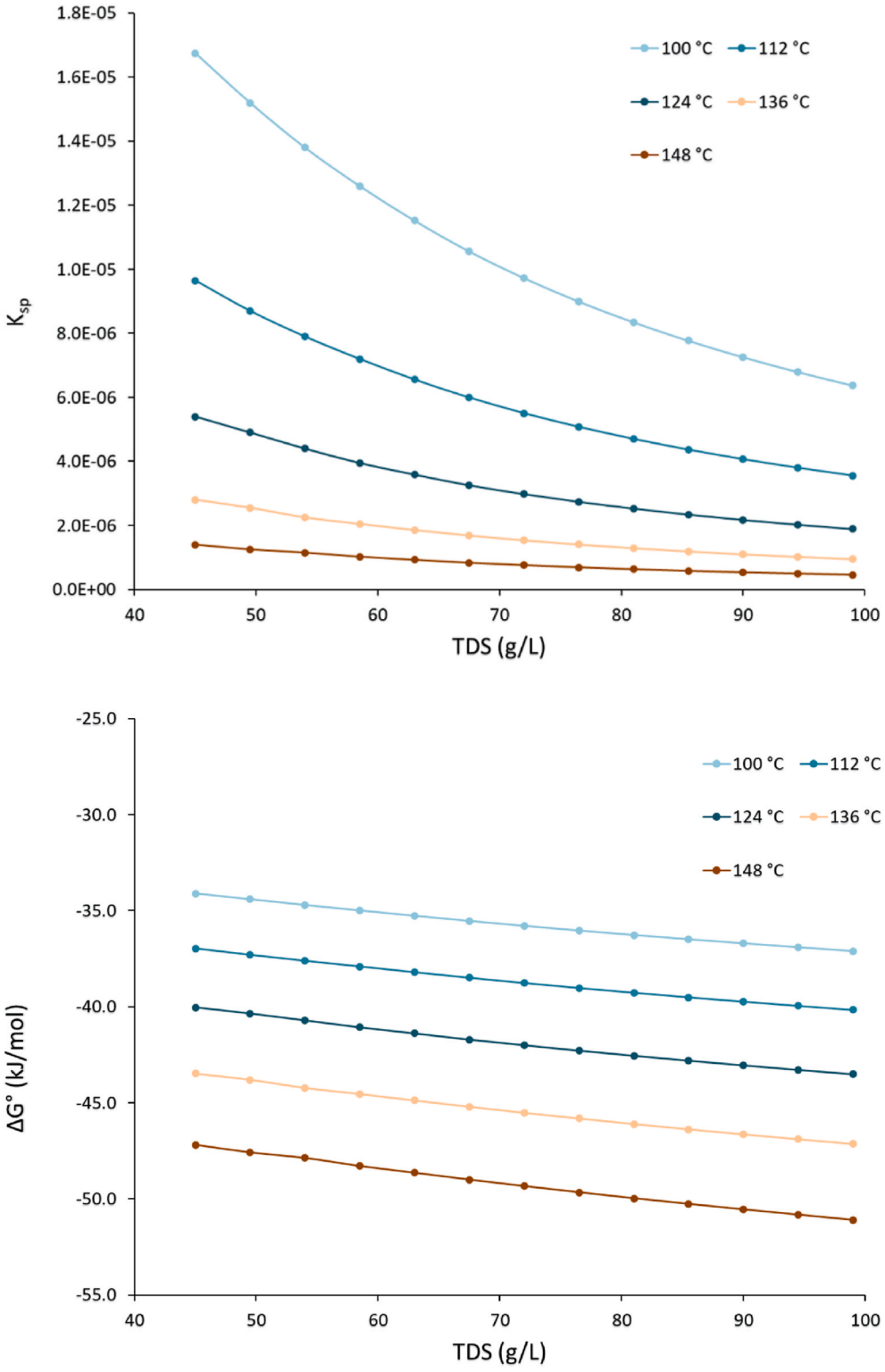

Fig. 3. Calculated solubility product K_{sp} of $CaSO_4.1/2H_2O$ and corresponding Gibbs free energy of precipitation at temperatures and concentrations of interest for MSF desalination.

$$SI = \ln\left(Q_{ip} \,/\, K_{sp}\right) = 61.5891 - 0.4783\ln(TDS) + 0.3223\left(\ln(TDS)\right)^2 - 31.7890\ln(T) + 3.7977\left(\ln(T)\right)^2 \quad \text{Eq. 18}$$

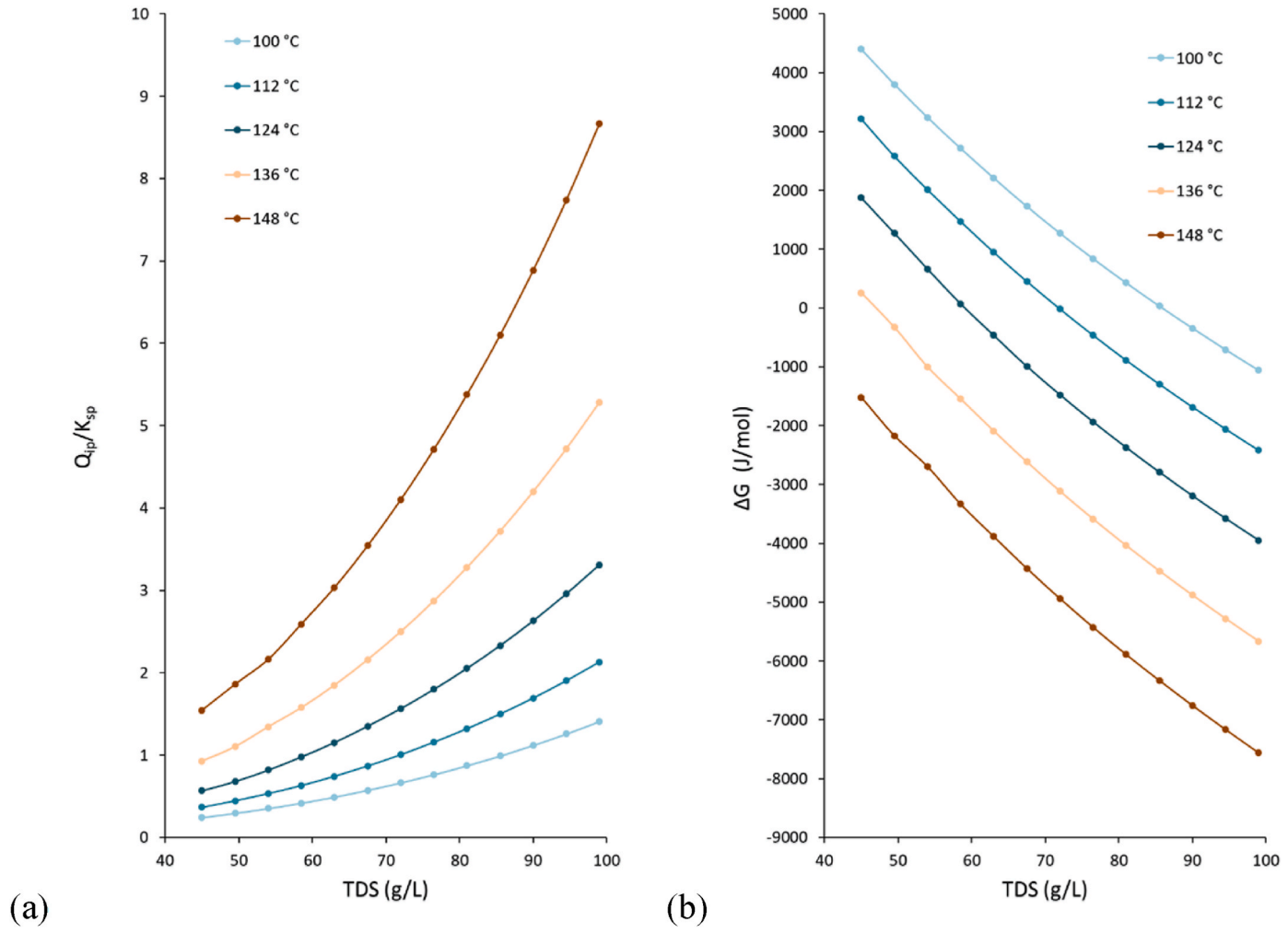

Fig. 4. Calculated (a) Supersaturation Q_{IP}/K_{sp}, and (b) Gibbs Free Energy of formation, ΔG, of $CaSO_4.1/2H_2O$ at temperatures and concentrations of interest for MSF desalination.

Table 4
Ratio of Q_{ip}/K_{sp} calculated by fitted expression Eq. (18) to Q_{ip}/K_{sp} calculated by application of Eqs. (1)–(17).

	Concentration (g/L)												
T (°C)	45	49.5	54	58.5	63	67.5	72	76.5	81	85.5	90	94.5	99
100	0.9977	0.9981	0.9999	0.9997	1.0018	1.0046	1.0058	1.0058	1.0050	1.0037	1.0020	1.0003	0.9984
112	1.0011	1.0081	1.0063	1.0046	1.0075	1.0100	1.0110	1.0108	1.0098	1.0083	1.0064	1.0045	1.0025
124	0.9865	0.9772	0.9823	0.9917	0.9935	1.0001	1.0011	1.0008	0.9996	0.9982	0.9962	0.9943	0.9920
136	0.9994	0.9814	0.9991	0.9893	0.9886	0.9909	0.9916	0.9909	0.9898	0.9883	0.9863	0.9841	0.9822
148	1.0146	1.010	0.9811	0.9927	0.9893	0.9917	0.9926	0.9917	0.9908	0.9885	0.9867	0.9843	0.9829

where TDS is measured in g/L and T in °C. The RMS relative error between values obtained by this Equation (18) from the values calculated from the full treatment of Eqs. (1)–(17) was 0.0096, with a maximum difference of 0.023 (Table 4).

A final caveat should be made to the extrapolation of expressions derived for pure calcium sulfate hydrates to the prediction of scaling in desalination systems. These scales are frequently compound, containing some calcium carbonate in addition to calcium sulfate even in the highest temperature environments [38], and as they are formed from a solution with a high concentration of sodium ions it is possible that significant doping of the calcium sulfate with sodium occurs [39]. In either case, differences in both the thermodynamics and kinetics of hard scale formation would be expected.

4. Conclusions

For the efficient operation of thermal desalination plants at high temperatures and concentration factors, it is necessary to avoid the precipitation of hard scale. This scale is predominantly calcium sulfate and forms first as calcium sulfate hemihydrate, $CaSO_4.½H_2O$. Application of solubility criteria determined at low ionic strength are not appropriate at the high ionic strengths at which hard scale forms in

Multi-Stage Flash (MSF) desalination. From solubility values appearing in the literature and the Pitzer model a semi-empirical expression for the supersaturation of calcium sulfate hemihydrate was determined for scaling limits as a function of brine temperature and total dissolved solids under the conditions applicable in MSF desalination. In this derived expression, the supersaturation index SI (equal to ln(*Qip*/*Ksp*)) is given by SI = 61.5891–0.4783 ln(TDS) + 0.3223 (ln(TDS))^2–31.7890 ln(T) + 3.7977 (ln(T))^2. The predictions of this expression were found to be consistent with the experience of plant operators in the MSF plants operated by the Saudi Water Authority. The Gibbs Free Energy, ΔG, was also determined for the first time for $CaSO_4.½H_2O$ formation under thermal desalination conditions.

CRediT authorship contribution statement

Ali Al-Hamzah: Writing – original draft, Project administration, Investigation, Formal analysis, Conceptualization. **Caillan J. Fellows:** Investigation. **Christopher M. Fellows:** Writing – review & editing, Formal analysis.

Funding Information

This work was carried out by the authors as paid work for the Saudi Water Authority, which covered all costs involved in the work.

Declaration of competing interest

The authors declare that they have no known competing financial interests or personal relationships that could have appeared to influence the work reported in this paper.

Appendix A. Supplementary data

Supplementary data to this article can be found online at https://doi.org/10.1016/j.cscee.2024.101088.

Data availability

Data will be made available on request.

References

[1] C.M. Fellows, A. Al-Hamzah, Thermal desalination: current Challenges, in: Z. Amjad, K. Demadis (Eds.), Mineral Scales and Deposits: Scientific and Technological Approaches, Elsevier, New York, 2015, pp. 583–602.
[2] T.A. Hoang, H.M. Ang, A.L. Rohl, Effects of temperature on the scaling of calcium sulphate in pipes, Powder Technol. 179 (2007) 31–37.
[3] B. Yu, S. Miao, M. Ding, Y. Ren, Solubility and Physical Properties of α-calcium sulfate hemihydrate in NaCl and Glycerol aqueous solutions at 303.15, 323.15, and 343.15 K, J. Chem. Eng. Data 66 (2021) 3686–3694.
[4] R. Taherdangkoo, M. Tian, A. Sadighi, T. Meng, H. Yang, C. Butscher, Experimental data on solubility of the two calcium sulfates gypsum and anhydrite in aqueous solutions, Data 7 (2022) 140.
[5] O.A. Hamed, A.M. Hassan, K. Al-Shail, K. Bamardouf, S. Al-Sulami, A. Hamza, M. A. Farooque, A. Al-Rubaian, Operational performance of an integrated NF/MSF desalination pilot plant'. Proc. International Desalination World Congress on Desalination and Water Reuse, Paradise Island, Bahamas, 23 .
[6] J. Glater, Evaluation of calcium sulfate scaling thresholds, in: Cooling Towers, a CEP Technical Manual, American Institute of Engineers, New York, 1972, pp. 138–145.
[7] J. D'Ans, The transition point between gypsum and anhydrite, Kali Steinsalz 5 (1968) 109–111.
[8] J. D'Ans, D. Bredtscheider, H. Eick, H.-E. Freund, Kali Steinsalz 9 (1953) 17–38.
[9] U. Sborgi, C. Bianchi, The solubilities, conductivities and X-ray analyses of anhydrous and semihydrated calcium sulphate, Gazz. Chim. Ital. 70 (1940) 823–835.
[10] A.E. Hill, The transition temperature of gypsum to anhydrite, J. Am. Chem. Soc. 59 (1937) 2242–2244.
[11] E. Bock, On the solubility of anhydrous calcium sulphate and of gypsum in concentrated solutions of sodium chloride at 25 °C, 30 °C, 40 °C, and 50 °C, Can. J. Chem. 39 (1961) 1746–1751.
[12] E. Posnjak, The system $CaSO_4$-H_2O, Am. J. Sci. 5 (1938) 247–272.
[13] K.U.G. Raju, G. Atkinson, The thermodynamics of 'scale' mineral solubilities. 3. Calcium sulfate in aqueous sodium chloride, J. Chem. Eng. Data 35 (1990) 361–367.
[14] D. Freyer, W. Voigt, Crystallization and phase stability of $CaSO_4$ and $CaSO_4$-based salts, Monatsh. Chem. 134 (2003) 693–719.
[15] S. Reigl, A.E.S. van Driessche, J. Mehringer, S. Koltzenburg, W. Kunz, M. Kellermeier, Revisiting the roles of salinity, temperature and water activity in phase selection during calcium sulfate precipitation, CrystEngComm 24 (2022) 1529–1536.
[16] E.P. Partridge, A.H. White, Solubility of calcium sulfate from 0 C to 200 °C, J. Am. Chem. Soc. 51 (1929) 360–370.
[17] A. Saha, J. Lee, S.M. Pancera, M.F. Bräu, A. Kempter, A. Tripathi, A. Bose, New insights into the transformation of calcium sulfate hemihydrate to gypsum using timer-resolved cryogenic transmission electron microscopy, Langmuir 28 (2012) 11182–11187.
[18] S. Polat, S, P. Sayan, Effects of tricarballylic acid on phase transformation of calcium sulfate hemihydrate to the dihydrate for', Cryst. Res. Technol. 52 (2017) 1600395.
[19] S. Reigl, A.E.S. van Driessche, E. Wagner, G. Montes-Hernandez, J. Mehringer, S. Koltzenburg, W. Kunz, M. Kellermeier, Toward more sustainable hydraulic binders: Controlling calcium sulfate phase selection via specific additives, ACS Sus, Chem. Eng. 11 (2023) 8450–8461.
[20] Y.W. Wang, F.C. Meldrum, Additives stabilize calcium sulfate hemihydrate (bassanite) in solution, J. Mater. Chem. 22 (2012) 22055–22062.
[21] O.A. Hamed, M.H. Ata, M.A. Farooque, K. Al-Shail, Performance analysis of trihybrid NF/RO/MSF desalination plant, Desal, Water Treat. 1 (2009) 215–222.
[22] A.M. Hassan, A.M. Farooque, A.T.M. Jamaluddin, A.S. Al-Amoudi, M.A.K. Al-Sofi, A. Rubian, M.M. Gurashi, N.M. Kither, A.G.I. Dalvi, I.A.R. Al-Tisan, Optimization of NF pretreatment of feed to seawater desalination plants, Int. Desalin. Water Reuse Q. 10 (2000) 45–46, 48.
[23] A. Al-Hamzah, C.M. Fellows, O.A. Hamed, Methallylsulfonate polymeric antiscalants for application in thermal desalination processes, Polymers 16 (2024) 2838.
[24] O.A. Hamed, Overview of hybrid desalination systems - current status and future prospects, Desalination 186 (2005) 207–214.
[25] K.S. Pitzer, Theoretical considerations of solubility with emphasis on mixed aqueous electrolytes, Pure Appl. Chemi. 58 (1986) 1599–1610.
[26] E. Rodil, J.H. Vera, Individual activity coefficients of chloride ions in aqueous solutions of $MgCl_2$, $CaCl_2$ and $BaCl_2$ at 298.2 K, Fluid Ph. Equilib. 187–188 (2001) 15–27.
[27] L.A. Cisternas, H.R. Galleguillos, Effects of temperature on activity coefficients in aqueous electrolyte solutions', AIChE J. 35 (1989) 1215–1218.
[28] S.H. Hashemi, M. Bagheri, S.A. Hashemi, Thermodynamic study of the effect of concentration and ionic strength on osmotic coefficient of aqueous sulfate and chloride solutions at 298.15 K', Model. Earth Syst. Environ. 6 (2020) 2189–2196.
[29] F. Millero, D. Pierrot, A chemical equilibrium model for natural waters, Aquat. Geochem. 4 (1998) 153–199.
[30] N. Møller, The prediction of mineral solubilities in natural waters: a chemical equilibrium model for the Na-Ca-Cl-SO_4-H_2O system, to high temperature and concentration, Geochim. Cosmochim. Acta 52 (1988) 821–837.
[31] UNESCO, Second Report of the Joint Panel on Oceanographic Tables and Standards, 1966, p. 4. Unesco Technical Papers in Marine Science, Paris.
[32] J.P. Greenberg, N. Møller, The prediction of mineral solubilities in natural waters: a chemical equilibrium model for the Na-K-Ca-Cl-SO_4-H_2O system to high concentration from 0 to 25 0°C', Geochim. Cosmochim. Acta 53 (1989) 2503–2518.
[33] D. Pierrot, F. Millero, L.N. Roy, R.N. Roy, A. Doneski, J. Niederschmidt, The activity coefficiencts of HCl in HCl−Na_2SO_4 solutions from 0 to 50 °C and ionic strengths up to 6 molal, J. Solution Chem. 26 (1997) 31–45.
[34] R. Sheikholeslami, H.W.K. Ong, Kinetics and thermodynamics of calcium carbonate and calcium sulfate at salinities up to 1.5 M, Desalination 157 (2003) 217–234.
[35] M.C. Simoes, K.J. Hughes, D.B. Ingham, L. Ma, M. Pourkashanian, Estimation of the Pitzer parameters for 1–1, 2–1, 3–1, 4–1, and 2–2 Single electrolytes at 25 °C, J. Chem. Eng. Data 61 (2016) 2536–2554.
[36] R. Zannoni, I. Resini, L. Liberti, M. Santori, G. Boari, Desulfation pretreatment for 138 Deg (280 DegF) operation: performance test of a 1 MGD plant at Doha East (Kuwait) power station, Desalination 66 (1987) 431–442.
[37] M.A. Al-Sofi, Fouling Phenomena in Multistage flash (MSF), Desalination 126 (1999) 61–76.
[38] A. Mubarak, A kinetic model for scale formation in MSF desalination plants. Effect of antiscalants', Desalination 120 (1998) 33–39.
[39] L. Wang, X. Li, Y. He, H. Huang, Y. Du, Doping behavior and occurrence state of Na impurity in α-calcium sulfate hemihydrate prepared in Na_2SO_4 solution, J. Crystal Growth 650 (2025) 127993.